

# Efficient waveguide mode extraction in white organic light emitting diodes using ITO-anodes with integrated MgF<sub>2</sub>-columns

Tobias Bocksrocker,<sup>1,\*</sup> Florian Maier-Flaig,<sup>1</sup> Carsten Eschenbaum,<sup>1</sup> and Uli Lemmer<sup>1</sup>

<sup>1</sup>Light Technology Institute, Karlsruhe Institute of Technology (KIT), Kaiserstr. 12, D-76131 Karlsruhe, Germany

\*[tobias.bocksrocker@kit.edu](mailto:tobias.bocksrocker@kit.edu)

We report a simple approach to enhance the out-coupling efficiency in white organic light emitting diodes (WOLEDs). By incorporating MgF<sub>2</sub>-columns into the ITO-anode and optimizing of their geometry, an overall efficiency enhancement of up to 38% is achieved. In addition, the structuring of the anode does not lead to a change in the electrical behaviour of the devices. As evidenced by goniometric measurements, the angular emission characteristics of the WOLEDs remain unchanged. Simulations, performed with the T-matrix method, reveal the effect of the enhanced outcoupling efficiency of this approach.

©2012 Optical Society of America

**OCIS codes:** (230.3670) Light-emitting diodes; (250.3680) Light-emitting polymers; (230.7390) Waveguides, planar.

---

## References and links

1. S. R. Forrest, "The road to high efficiency organic light emitting devices," *Org. Electron.* **4**(2-3), 45–48 (2003).
2. N. Patel, S. Cina, and J. Burroughes, "High-efficiency organic light-emitting diodes," *IEEE J. Sel. Top. Quantum Electron.* **8**(2), 346–361 (2002).
3. C.-C. Wu, C.-W. Chen, C.-L. Lin, and C.-J. Yang, "Advanced organic light-emitting devices for enhancing display performances," *J. Disp. Technol.* **1**(2), 248–266 (2005).
4. M. C. Gather, A. Köhnen, and K. Meerholz, "White organic light-emitting diodes," *Adv. Mater. (Deerfield Beach Fla.)* **23**(2), 233–248 (2011).
5. H. Kim, C. Gilmore, A. Pique, J. S. Horwitz, H. Mattoussi, H. Murata, Z. H. Kafafi, and D. B. Chrisey, "Electrical, optical, and structural properties of indium-tin-oxide thin films for organic light-emitting devices," *J. Appl. Phys.* **86**(11), 6451–6461 (1999).
6. R. T. Chen and D. Robinson, "Electro-optic and all-optical phase modulator on an indium tin oxide single-mode waveguide," *Appl. Phys. Lett.* **60**(13), 1541–1543 (1992).
7. K. Saxena, V. K. Jain, and D. S. Mehta, "A review on the light extraction techniques in organic electroluminescent devices," *Opt. Mater.* **32**(1), 221–233 (2009).
8. S. Möller and S. Forrest, "Improved light out-coupling in organic light emitting diodes employing ordered microlens arrays," *J. Appl. Phys.* **91**(5), 3324–3327 (2002).
9. J. Zhou, N. Ai, L. Wang, H. Zheng, C. Luo, Z. Jiang, S. Yu, Y. Cao, and J. Wang, "Roughening the white OLED substrate's surface through sandblasting to improve the external quantum efficiency," *Org. Electron.* **12**(4), 648–653 (2011).
10. J. Hauss, T. Bocksrocker, B. Riedel, U. Lemmer, and M. Gerken, "On the interplay of waveguide modes and leaky modes in corrugated OLEDs," *Opt. Express* **19**(S4 Suppl 4), A851–A858 (2011).
11. U. Geyer, J. Hauss, B. Riedel, S. Gleiss, U. Lemmer, and M. Gerken, "Large-scale patterning of indium tin oxide electrodes for guided mode extraction from organic light-emitting diodes," *J. Appl. Phys.* **104**(9), 093111 (2008).
12. B. Riedel, J. Hauss, M. Aichholz, A. Gall, U. Lemmer, and M. Gerken, "Polymer light emitting diodes containing nanoparticle clusters for improved efficiency," *Org. Electron.* **11**(7), 1172–1175 (2010).
13. Y. Sun and S. Forrest, "Enhanced light out-coupling of organic light-emitting devices using embedded low-index grids," *Nat. Photonics* **2**(8), 483–487 (2008).

---

## 1. Introduction

Organic light emitting diodes (OLEDs) have been of great interest in research as well as in industrial development over the last years [1–3]. The main advantages are their low energy consumption, good color qualities and Lambertian emission characteristic. These properties and the potentially low-cost manufacturing also render white OLEDs (WOLEDs) as a very promising light source for general lighting [4].

A typical OLED consists of an ITO anode, several thin layers of different organic materials and a metallic cathode. OLEDs are typically built on glass substrates. The standard thickness of the ITO anode and the organic materials is in the range of ~200 nm. The refractive index of ITO is 1.8 – 2.1 (depending on the processing and treatment) [5,6], typical organic materials used in OLEDs possess a refractive index of 1.7 – 2.0. Since the adjacent materials (glass, air, metal) have lower refractive indices, the OLED-stack forms a slab waveguide. As a significant part of the intensity profile is located in the active layer, light generated in the electroluminescent device can couple to waveguide modes and surface plasmon polaritons thereby no leading to the desired light emission in forward direction. These optical losses add up to about 50% [7]. Another 30% of the generated light is coupled into substrate modes which rely on the total internal reflection at the glass/air interface [7]. Substrate modes can be relatively easily extracted, *e.g.*, by structuring the glass/air interface with microlenses or (randomly) roughening the glass surface [8,9]. Extraction of waveguide modes is more complicated, due to the thin layers used in OLEDs. Most of the published approaches have disadvantages for the application in white OLEDs: Periodic structures, such as Bragg-gratings show an angular spectral shift of the light emission [10,11]. Other approaches to couple out waveguide modes can change the electrical behavior [12] of the device or require a complex processing [13].

In our study we implemented  $\text{MgF}_2$ -columns in the ITO-anode of WOLEDs in order to couple out waveguide modes, without changing the electrical behaviour or influencing the angular emission characteristics of the device. We observe an efficiency increase of up to 38% by using an up-scalable method.

## 2. Fabrication

### 2.1 $\text{MgF}_2$ -column fabrication

$\text{MgF}_2$ -columns integrated in the ITO-anode were fabricated by standard photo-lithography with a subsequent wet etching process and an evaporation step. Figure 1 shows the fabrication scheme of the  $\text{MgF}_2$ -columns integrated in the ITO-anode. As a starting point we used a 1 mm thick glass substrate covered with a 120 nm thick ITO layer. After cleaning with acetone and isopropyl alcohol respectively, in an ultrasonic bath for 10 min each, the ITO-substrates were treated in an oxygen plasma for 2 min. As an adhesive layer for the following photoresist, TI prime (from MicroChemicals GmbH) was spun at 3000 rpm for 20 s onto the substrate followed by a subsequent curing at 100°C for 2 min. As a photoresist a layer of ma-p 1215 (purchased from micro resist technology GmbH) was spun at 2000 rpm for 30 s resulting in a 1.2  $\mu\text{m}$  thick layer (Fig. 1(a)). After a prebake at 100°C for 90 s, the column structure was exposed to the photoresist via a standard lithography process (Fig. 1(b)). After developing the resist with the developer ma-D 331 (Fig. 1(c)), the substrates were immersed into hydrochloric acid for 7 min, etching off the ITO at the exposed locations (Fig. 1(d) and Fig. 1(e)). After stopping the etching process with  $\text{H}_2\text{O}$ , an  $\text{MgF}_2$  layer was evaporated under vacuum ( $\sim 5 \cdot 10^{-6}$  mbar) on top of the substrates (Fig. 1(f)). After a lift-off process with acetone (Fig. 1(g)) the substrate was cleaned with isopropyl alcohol to remove any residues from the photoresist. In the following subsection, the fabrication of the OLEDs is described (Fig. 1(h)).

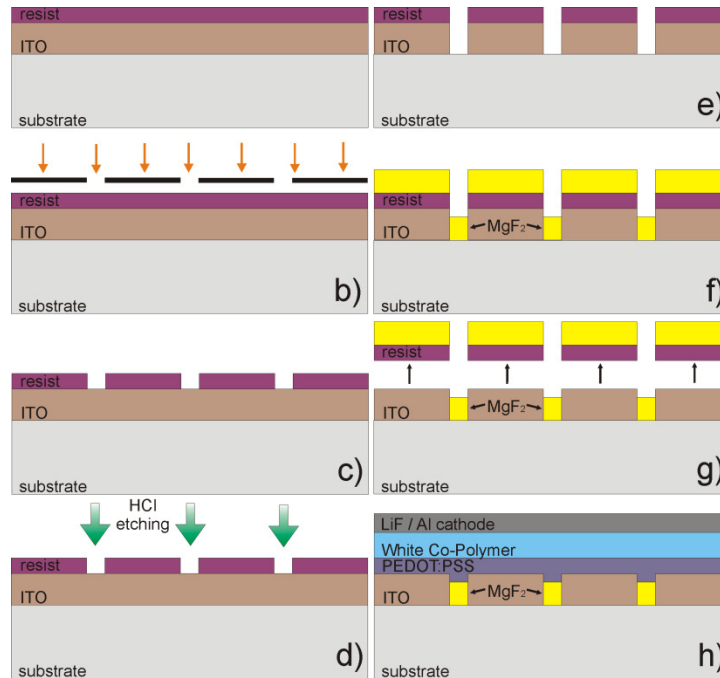


Fig. 1. Schematic of the processing steps for  $\text{MgF}_2$ -columns incorporated in ITO-anodes. (a) A photoresist layer is spincoated on an ITO-covered glass substrate. (b) The column structure is exposed into the resist. (c) Development of the photoresist. (d) Column-structure is wet-etched with HCl into the ITO using the resist as an etching mask. (e) Column bowls are resulting in ITO. (f)  $\text{MgF}_2$  is evaporated onto the substrate. (g) A lift-off is performed with acetone. (h) A white polymer-OLED is fabricated on the column structured ITO.

## 2.2 OLED fabrication

For the reference device, planar unstructured ITO was used. The reference and the  $\text{MgF}_2$ -columns structured ITO substrates were cleaned with acetone and isopropyl alcohol respectively, in an ultrasonic bath, before they were treated with oxygen plasma to increase the workfunction of the ITO and to remove any residues from the solvents. The WOLED stack was fabricated in a nitrogen atmosphere according to the following procedure. A layer of Poly(3,4-ethylenedioxythiophene):poly(styrenesulfonate) (PEDOT:PSS, "Baytron P VPAI 4083", purchased from H. C. Starck, diluted with  $\text{H}_2\text{O}$  in a ratio of 1:1) was spincoated at 4000 rpm resulting in a  $\sim 20$  nm thick layer. A white light emitting co-polymer from Merck OLED Materials GmbH (SPW093) was used as the active layer. The material was dissolved in toluene at a weight/volume ration of 6 mg/ml, and spun on at 1000 rpm resulting in a  $\sim 70$  nm thick layer. As a cathode, 1 nm LiF and 200 nm Al was evaporated under vacuum ( $\sim 10^{-7}$  mBar). The substrates contained four active areas, each with a size of 5 mm x 5 mm. The OLEDs were then encapsulated with an epoxy resin adhesive and a glass cover to perform characterization under ambient conditions.

## 3. Measurement and results

To compare the overall efficiency of the structured and the reference devices, an integrating sphere was used. A multimode fiber was coupled to a spectrometer (Acton Research Corporation SpectraPro-300i) with an attached ICCD-camera (Princeton Instruments PiMax:512). As a power supply for the OLEDs and to simultaneously obtain the I-V-characteristic of the devices, a source-measure unit (Keithley SMU 236) was used. To investigate any changes in the emissive characteristics of the devices, goniometric measurements were performed. A multimode fiber (coupled to the same spectrometer as the

integrating sphere) was held at a fixed point. The OLEDs were driven by a constant current supplied by a Keithley SMU 236, and then rotated with respect to fiber, which allows recording of the angle resolved emission of the devices.

Different parameters were varied to optimize the outcoupling structures. Keeping the diameter of the columns fixed at  $2.5\ \mu\text{m}$ , we built devices with a distance in between the columns of  $5\ \mu\text{m}$ ,  $10\ \mu\text{m}$  and  $15\ \mu\text{m}$ . For each of the different distances we varied the column height, so that heights of  $33\ \text{nm}$ ,  $66\ \text{nm}$  and  $100\ \text{nm}$  were investigated. Figure 2(a) shows the overall efficiency enhancement (in terms of luminous flux normalized to the electrical power consumption) of the devices in correlation with the different column distances and heights, compared to the reference devices with an unstructured ITO anode.

A maximum efficiency enhancement of 38% is obtained for a column distance of  $5\ \mu\text{m}$  and a column height of  $66\ \text{nm}$ . The efficiency enhancement can be explained by the drastic change of the refractive index within the ITO, due to the structuring with  $\text{MgF}_2$ . ITO has a refractive index of  $1.8 - 2.1$ ,  $\text{MgF}_2$  has a refractive index of  $1.38$ .

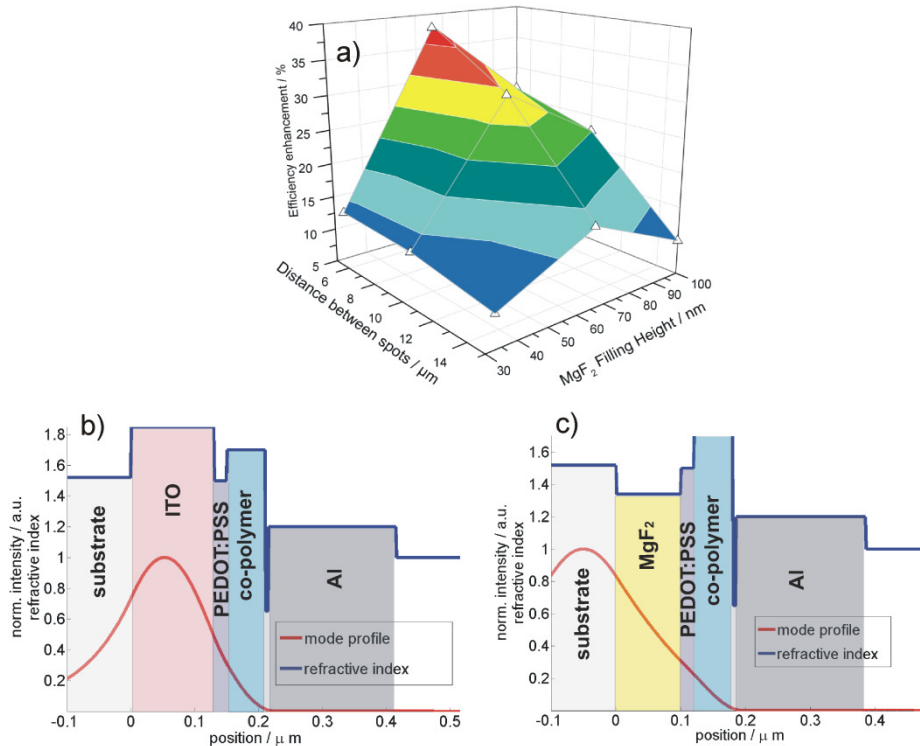


Fig. 2. (a) Measured efficiency enhancement with different column distances and heights. (b) T-Matrix simulation of the waveguide mode at 450 nm distribution at the position of ITO. (c) T-Matrix simulation of the waveguide at 450 nm mode distribution at the position of  $\text{MgF}_2$ . The waveguide mode is shifted towards the substrate.

Simulations performed with the transfer matrix method showed, that in the corresponding slab waveguide used to model the optical behavior of the OLED, the light essentially propagates in the ITO anode (high filling factor in the ITO, see Fig. 2(b)). The simulations shown in Fig. 2(b) and Fig. 2(c) were performed at a wavelength of  $450\ \text{nm}$ . This wavelength was chosen exemplarily, other wavelengths yielded qualitatively similar results. The outcoupling effect due to a perturbed waveguide is expected to be very efficient, when the ITO is replaced by a low-index material. At the position of the  $\text{MgF}_2$ , no guided mode exists such that the guided mode from the surrounding areas can couple to substrate modes or propagating modes (Fig. 2(c)). Hence, the extraction efficiency is enhanced by this scattering process.

Adding such a low-index structure into the anode might also change the electrical behaviour of the device, due to changes in the sheet resistance, loss of active area ( $\text{MgF}_2$ -columns might not be considered as “active area”, since  $\text{MgF}_2$  is an insulator) or due to corrugation of the organic layers. However, no change in the sheet resistance was observed. We explain this due to the small size of the columns in comparison to the remains of the ITO. Figure 3(a) shows exemplarily the very similar current-density characteristics of the devices with a column height of 66 nm and a column distance of 5  $\mu\text{m}$ , 10  $\mu\text{m}$  and 15  $\mu\text{m}$ . The effect of the efficiency enhancement cannot be explained by these small deviations, since the efficiency of the devices were compared at a fixed power consumption, not at a certain current density.

Furthermore  $\text{MgF}_2$ -column structures do not lead to a change in the angular and spectral emission properties of the WOLEDs. Figure 3(b) shows exemplarily the normalized spectra of the reference device and the devices with column distances of 5  $\mu\text{m}$ , 10  $\mu\text{m}$  and 15  $\mu\text{m}$  at a viewing angle of  $40^\circ$ .

No noteworthy changes in the emission spectra are observed. Thus the enhancement covers the whole spectrum uniformly, since no preferred wavelength was observed. The inset in Fig. 3(b) shows the unchanged angle resolved emission at a wavelength of 520 nm. In contrast to approaches based on diffraction grating, the structuring of the ITO-anode with  $\text{MgF}_2$ -columns is therefore attractive for the application in WOLEDs, since it does not influence the spectral and angular emission characteristic of the devices.

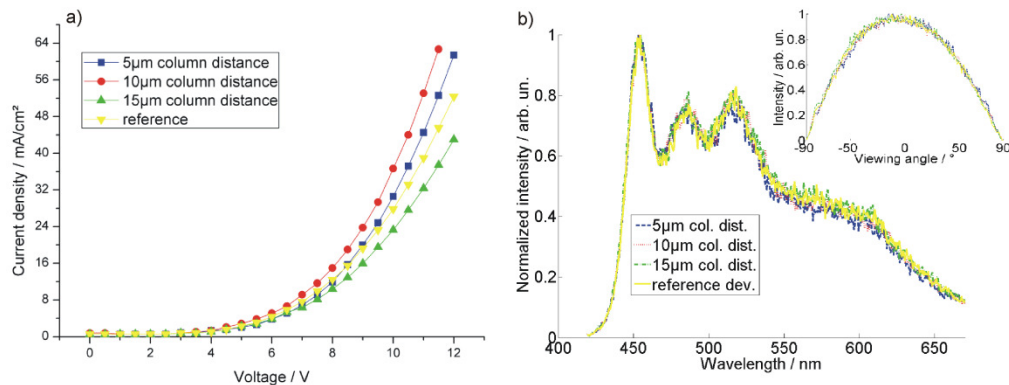


Fig. 3. (a) Current-density characteristics of devices with different column distances and a column height of 66 nm. (b) Emission spectra at a viewing angle of  $40^\circ$ . The inset shows the angle resolved emission at a wavelength of 520 nm.

#### 4. Conclusion

In conclusion, we presented a method to structure ITO anodes in white OLEDs with  $\text{MgF}_2$ -columns. The  $\text{MgF}_2$  columns significantly enhance the outcoupling of guided modes in the device and therefore increase the overall efficiency of the devices of up to 38% while the angular and spectral emission characteristics and the electrical behaviour remain unchanged.

#### Acknowledgments

The authors would like to thank Merck OLED Materials GmbH for material supply.